Epidemic Hemorrhagic Fever

15

Bailu Liu, Jinling Zhang, and Han Huang

Epidemic hemorrhagic fever (EHF), also known as hemorrhagic fever with renal syndrome (HFRS), is an acute infectious disease with natural epidemic focus, which is caused by epidemic hemorrhagic fever virus (EHFV). So far, a total of 13 types of human viral hemorrhagic fever have been identified. Based on presence of renal lesions, the disease is categorized into two types: hemorrhagic fever with renal lesion and hemorrhagic fever with no renal lesion. EHF is mainly distributed in Eurasia, but EHFV spreads throughout the world. In China, epidemics of EHF continually occur for more than 70 years, which is the second most serious health-threatening viral infection following viral hepatitis.

15.1 Etiology

15.1.1 Classification of EHFV

Epidemic hemorrhagic fever virus, the pathogen of EHF, is categorized into the genus of Hantavirus (HV) and the family of Bunyaviridae. With the development and application of molecular biological techniques, HV has been discovered with around 30 genotypes all over the world, among which Hantaan virus (HTNV), Seoul virus (SEOV), Puumala virus (PUUV), and Dobrava-Belgrade virus (BDOV) are pathogenic. In China, EHF is mainly caused by HTNV and SEOV.

B. Liu (✉)
CT Department, Harbin Medical University, Harbin, Heilongjiang, China
e-mail: liubailuhmu@sina.com

J. Zhang
CT Department, The Second Affiliated Hospital, Harbin Medical University, Harbin, Heilongjiang, China

H. Huang
Department of Radiology, The third People's Hospital, Harbin, Heilongjiang, China

15.1.2 HV Genome Structure and Its Properties

Under an electron microscope, HV is demonstrated with characteristic polymorphism. HV is usually medium-sized particle, with an average diameter of approximately 120 nm (90–160 nm). The virus has double envelopes, with peplomers in the outer membrane and granular and linear structure inside the envelope. Generally, the cytoplasm in infected cells is demonstrated with multiple characteristic inclusion bodies. Relevant experiments have proved that gene rearrangement may occur between HTNV and SEOV.

15.1.3 HV Structural Protein and Its Properties

The nucleoprotein of HV has relatively strong immunogenicity and steady antigenic determinants. It is generally acknowledged that HV nucleoprotein contains alexofixagens, but does not contain neutralizing antigen. After the host is infected by HV, the firstly detected antibody is nucleoprotein antibody and it can be detected at day 2–3 of the whole illness course, which facilitates the early diagnosis.

15.1.4 Physical and Chemical Properties of HV

HV has weak resistance to external environment and is relatively stable at a temperature of 4–20 °C. It can be inactivated at a temperature of above 37 °C or at an environment with a pH value lower than 5.0. In addition, it is quite sensitive to deoxycholate and some lipid solvents like ether, chloroform, and acetone, and it can be inactivated by radiation of ultraviolet and gamma ray as well as common disinfectants.

H. Li (ed.), *Radiology of Infectious Diseases: Volume 1*, DOI 10.1007/978-94-017-9882-2_15

15.2 Epidemiology

15.2.1 Host Animals and Source of Infection

Since EHF is an acute infectious disease with natural epidemic focus, its occurrence is related to infection during field activities. In China, striped field mice act as the main host animals and source of infection of field mouse hemorrhagic fever. Sewer rats act as the main host animals and source of infection of house mouse hemorrhagic fever in China and urban hemorrhagic fever in both Japan and Korea. Korean field mice act as the main host animals and source of infection of forest hemorrhagic fever in China.

15.2.2 Route of Transmission

Concerning the routes of transmission of EHF, various theories have been proposed with no agreement. Generally, it has been acknowledged that its routes of transmission can be categorized into three types: animal-borne transmission (including transmissions via skin wounds, respiratory tract, and digestive tract), arthropod-borne transmission (such as mite), and vertical transmission. The direct transmission from mouse to human is an important route for its spread to human.

15.2.3 Susceptible Population

People are generally susceptible to HV, but the onset of EHF depends on the type of infected virus. The disease more commonly occurs in young adults, especially farmers and field workers. Males are more vulnerable to the disease than females. And pediatric patients are extremely rare. After the onset, the serum antibody can reach the peak within 2 weeks and persist for a long period of time afterward. After 2–3 weeks, the serum antibody begins to decrease. After its infection, lifelong immunity against the disease can be acquired and the repeated infection is extremely rare.

15.2.4 Epidemiological Features

15.2.4.1 Types of Disease and Regional Distributions

EHF occurs worldwide, especially in those coastal cities, which is widely transmitted via mice. Thus, it has been a global public health issue. In China, by the means of etiological and serological tests, it has been proved that EHF prevails throughout 26 provinces (cities, regions). In recent years, prevalence of house mouse hemorrhagic fever has rapidly been extending the epidemic area into big, medium, and coastal cities, which has been recognized as an urgent and serious threat to the public health.

15.2.4.2 Seasonal Distribution

In China, EHF can occur all over a year, whose prevalence is characterized by highly sporadic throughout a year. However, in most epidemic areas, seasonal prevalence does obviously exist. The incidence peak of field mouse hemorrhagic fever is usually found in autumns, while that of house mouse hemorrhagic fever occurs mainly in springs and early summers, with a more common occurrence during the period from March to June.

15.2.4.3 Epidemic Periodicity

The prevalence of EHF is periodic, namely, an incidence peak at certain season or an incidence peak after certain years.

15.3 Pathogenesis and Pathological Changes

15.3.1 Pathogenesis

So far, the pathogenesis of EHF has not been fully understood. Most studies have demonstrated that HV is the initial factor to trigger the onset of EHF. On the one hand, the infection of HV can cause destructed structure and functions of the infected cells. On the other hand, the infection of HV can also induce immune response of the host and release of various cytokines, which contribute to elimination of some HV for protection against further damages. However, it also plays a role in damaging organs and tissues in human body. All of these can lead to cell degeneration, necrosis, and even apoptosis, which can further impair organ functions. In addition, due to the pantropic infection of HV to human body, multiple organ lesions can be caused.

15.3.2 Pathological Changes

The pathological lesions caused by EHF can be quite extensive, possibly with different degrees of pathological changes occurring in each system and organ of the host. Lesions of congestion, hemorrhage, and edema are diffusely distributed in the skin, mucosa, tissues, and organs, even with necrosis in some severe cases. The most apparent changes can be found in the kidney medulla, right atrial endocardium, anterior pituitary, and adrenal cortex, with the following main manifestations.

15.3.2.1 Pervasive Systemic Microvascular and Capillary Lesions

The endothelial cells of the systemic small vessels (including arterioles, venules, and capillaries) are subject to swelling, degeneration, and necrosis. The vascular walls are subject to irregular contracts and dilations, with finally occurrence of fibrinoid necrosis. Accompanying microthrombus may be found in the disintegrated lumen.

15.3.2.2 Multifocal Hemorrhage

Extensive hemorrhages can be found in the skin and mucosa as well as organs and tissues of the whole body. Organ hemorrhages are most obvious at the interface of renal cortex and medulla, under the right atrial endocardium, in the gastric mucosa, and in the anterior pituitary, which can be observed immediately in the febrile stage. Organ hemorrhage is most obvious in the oliguria stage.

15.3.2.3 Severe Exudation and Edema

In the early stage of the disease, edemas occur in the bulbar conjunctiva and eyelid, with the following different degrees of edema and effusion in different organs and body cavities. Edema and effusion are most serious in the retroperitoneum, mediastinum, lungs, and other loose tissues. During the oliguria stage, the conditions can be complicated by pulmonary edema and cerebral edema.

15.3.2.4 Focal Necrosis and Inflammatory Cell Infiltration

Coagulative necrosis lesions can be found in most organs, tissues, and parenchyma cells, especially in the kidney medulla, anterior pituitary, the intermediate area of hepatic lobules, and adrenal cortex. In addition, infiltration of monocytes and plasmocytes can be observed in the lesions.

15.3.2.5 Extensive Formation of Microthrombus

In addition to typical thrombus, microthrombi composed of fibrins can be found in the capillaries, which serve as a histological evidence supporting the occurrence of DIC during the pathogenesis of EHF.

15.3.3 Pathological Changes of Major Organs

15.3.3.1 Kidney

By naked eyes, edema and hemorrhage of the renal adipose capsule can be observed. The renal cortex is ischemic and pale, while the renal medulla is extremely congestive, with accompanying edema and hemorrhage. By microscopic examination, the glomerulus is subject to congestion, thickening of the basilar membrane, degenerated renal proximal tubule, and narrowed or occlusive renal tubule due to compression as well as infiltration of cells in the renal interstitium.

15.3.3.2 Heart

By naked eyes observation, extensive hemorrhage can be found under the right atrial endocardium, which may infiltrate into the whole myocardium and even under the pericardium. Subendocardial hemorrhages also can be found in the cardiac muscle, valves, and arteries. Under a microscope, myocardial interstitium is subject to hemorrhage, with a small quantity of infiltration of inflammatory cells as well as different degrees of degeneration, necrosis, and breakage of myocardical fibers.

15.3.3.3 Pituitary Gland

By naked eyes observation, the pituitary gland is subject to slight swelling, grayish red color, as well as congested and hemorrhagic capsule. The neurohypophysis has no obvious changes. Under a microscope, remarkable congestion, hemorrhage, and coagulative necrosis can be observed in the anterior pituitary.

15.3.3.4 Adrenal Gland

The changes are pathologically characterized by adrenal edema, enlarged volume, as well as tense, congested, and hemorrhagic capsule. Under a microscope, the cortex is reticular with necrotic foci, and sebaceous gland cells are subject to vacuolar degeneration. In addition, obvious lipoid loss can be observed, with intravascular formation of microthrombi.

15.3.3.5 Respiratory System

Scattered hemorrhagic spots can be found in the trachea and bronchi, and under a microscope, extremely dilated capillaries and blood stasis in the alveolar wall, partially with microthrombus. Large quantities of exudative plasmocytes and erythrocytes can be observed in the pulmonary alveolar cavities.

15.3.3.6 Digestive System

Diffuse hemorrhage can be found in the gastric mucosa, with scattering hemorrhagic spots in the duodenum and superior jejunum and obviously less hemorrhagic spots in the colon and inferior small intestine. The hepatocytes are subject to steatosis, with scattering focal necrosis. Retroperitoneal gelatinous edema is a characteristic change in cases of EHF.

15.4 Clinical Symptoms and Signs

The incubation period of EHF generally lasts for 1–2 weeks. The typical cases show an acute onset, with three main symptoms of fever, hemorrhage, and renal lesion. Based on severity of the conditions, it can be categorized into four types: mild, moderate, serious, and critical types of EHF. The whole illness course can be divided into five stages: febrile, hypotensive shock, oliguria, diuresis, and convalescence stages.

15.4.1 Febrile Stage

The clinical manifestations at this stage resemble to serious cold, mostly with an acute onset, sudden aversion to cold, and fever with the body temperature reaching up to 39–40 °C within 1–2 days. The fever is mostly remittent and continued, usually lasting for 3–7 days, with accompanying headache, severe lower back pain, and orbital pain (namely, the

three pains). Some patients may experience nausea, vomiting, abdominal pain, and diarrhea. In severe cases, the patients may even experience drowsiness, irritation, and delirium. After the body temperature returns to normal, the systemic toxic symptoms are not alleviated but possibly aggravated, which is a characteristic clinical manifestation of EHF.

The main physical signs of EHF include flushing skin in the face, neck, and upper chest with a drunken-like appearance, namely, the triple skin flushing sign, which is an important early sign of EHF and has value for the early diagnosis. Another important early sign of EHF, the triple mucosa sign, manifested as congested and red ocular conjunctiva, oral soft palate, and postpharyngeal wall mucosa, with multiple small spots of hemorrhage. Within 2–3 days after the onset, the patients experience apparent exudative edema possibly with hemorrhagic spots and ecchymosis as well as conjunctival edema. Meanwhile, the patients may also experience skin hemorrhagic spots, which are in scattering or clustering distribution or appear like scratching or cord-like. Some patients with serious conditions may also experience ecchymoses and petechiae all over the body, with nasal bleeding, hemoptysis, or tract bleeding, mostly caused by DIC.

15.4.2 Hypotensive Shock Stage

Hypotensive shock stage is characterized by normal body temperature but aggravated conditions. The main clinical manifestations include cardiovascular toxic symptoms occurring after fever persisting for 4–6 days when the body temperature returns to normal or shortly after the body temperature returns to normal. The patients experience decreased blood pressure, increased heart rate, terminal limb coldness, less volume of urination, irritation, disturbance of consciousness, drowsiness or lethargy that gradually develops into coma, cyanosis in the lips and extremities, shortness of breath, and increased hemorrhage. This stage usually lasts for 1–3 days and possibly even above 6 days in some serious cases. In some patients, the symptoms of this stage are inapparent and the patients may rapidly develop into oliguria or diuresis stage.

15.4.3 Oliguria Stage

Mostly, the oliguria stage begins at day 5–8 of the whole illness course and usually lasts for 2–5 days. In some serious cases, oliguria persists for 1 week. The severity of conditions during this stage is parallel to oliguria and azotemia, with clinical manifestations of poor appetite, nausea, abdominal distension, dizziness and headache, large areas of skin ecchymoses, deep and rapid breathing, weak cardiac contractility, and decreased blood pressure. Sometimes, the patient may also experience hypervolemia syndrome. In some severe cases, the patients experience heart failure, pulmonary edema, and cerebral edema. Meanwhile, the tendency of hemorrhage is more obvious during this stage.

15.4.4 Diuresis Stage

The diuresis stage usually begins at day 9–14 of the whole illness course, commonly lasting for 1–2 weeks. In some rare serious cases, this stage may persist for several months, with occurrence of various secondary infections. During this stage, the renal lesions are gradually healed, with obviously increased volume of urination, which may reach up to above 3000 ml within 24 h, and the recorded maximal volume is 20,000 ml within 24 h. Early at this stage, there is usually a migrating period from oliguria stage to the diuresis stage, which commonly persists for 3–5 days.

15.4.5 Convalescence Stage

After 3–4 weeks of the disease, the patients develop into the convalescence stage, with gradual absence of main clinical symptoms. Along with the gradual recovery of the renal functions, the volume of urination decreases to less than 3000 ml within 24 h. Most patients are cured after 1–3 months.

15.5 Epidemic Hemorrhagic Fever-Related Complication

15.5.1 Hemorrhage

The most common hemorrhages are hematemesis and hematochezia, which can induce secondary shock. In addition, abdominal hemorrhage, nasal bleeding, and vaginal bleeding are also relatively common.

15.5.2 Adult Respiratory Distress Syndrome

Adult respiratory distress syndrome mostly occurs in the hypotensive shock and oliguria stages. The patients experience chest distress and shortness of breath with a respiratory rate of 30–40 times per minute. By physical examination, dry and moist rales can be heard in the lungs. By blood gas

analysis, arterial partial pressure of oxygen can be found with obvious decrease.

15.5.3 Complications of the Central Nervous System

The complications of the central nervous system include encephalitis and meningitis caused by invasion of EHFV into the central nervous system in the early stage. In addition, they also include cerebral edema, hypertensive encephalopathy, and intracranial hemorrhage due to shock, coagulation disorders, electrolyte disturbance, and hypervolemia syndrome in the hypotensive shock and oliguria stages. The patients may experience headache, vomiting, disturbance of consciousness, convulsion, changed respiratory rhythm, or hemiplegia.

15.5.4 Cardiac Insufficiency and Pulmonary Edema

Cardiac insufficiency and pulmonary edema commonly occur in the hypotensive shock and oliguria stages, with a sudden onset within a short period of time and serious conditions. The patients experience obvious hypervolemia syndrome. Due to overload of myocardium induced by hypervolemia syndrome and pulmonary edema, heart failure may occur.

15.5.5 Idiopathic Renal Rupture

It commonly occurs in the oliguria stage, which is caused by severe renal medulla hemorrhage. The patients mostly experience sudden increase of abdominal or thoracic pressures due to nausea, vomiting, or cough. The consequent occurrence of increased nephrovascular pressure promotes hemorrhage. Clinically, the patients may experience sudden and severe lower back or abdominal pain and even decreased blood pressure and cold sweat in some serious cases. In cases with leakage of blood into the abdominal cavity, peritoneal irritation signs can be found. By abdominal cavity puncture, fresh blood can be observed.

15.5.6 Other Complications

Other complications of EHF include secondary infections, which are mostly pulmonary infection, urinary system infection and septicemia, uremic pericarditis, pericardial effusion, and hyperosmolar nonketotic coma.

15.6 Diagnostic Examination

15.6.1 Laboratory Test

15.6.1.1 Routine Examination

Routine Blood Test

At different stages of the disease, routine blood test shows different results, which are important for both diagnosis and predicting prognosis.

Routine Urine Test

By routine urine test, obvious urine protein is an important sign of the disease, which is also the earliest sign of renal lesions.

Routine Stool Test

In the early stage of gastrointestinal bleeding, most cases show positive occult blood test.

15.6.1.2 Blood Biochemical Examination

Both blood urea nitrogen and creatinine can be detected with mild or moderate increase in the hypotensive shock stage, which increase to their peaks during the oliguria stage and the diuresis stage. Afterward, their levels begin to decrease. The degree and speed of increase are positively related to the severity of the conditions. By blood gas analysis, respiratory alkalosis is relatively common in the febrile stage while metabolic acidosis is more common in the hypotensive shock and oliguria stages. Serum sodium, chlorine, and calcium mostly decrease in each stage of the disease, while serum phosphorus and magnesium increase. Serum potassium remains at low level in the febrile and hypotensive shock stages, which increases in the oliguria stage but decreases again in the diuresis stage.

15.6.1.3 Liver Function Test

In about 50 % of the patients, alanine transaminase (ALT) can be detected with an increase. In some rare patients, serum bilirubin is detected also with an increase.

15.6.1.4 Blood Coagulation Function Test

The blood platelet level begins to decrease at day 2 of the disease, which reaches its lowest level in the hypotensive shock and oliguria stages.

15.6.1.5 Immune Function Test

Specific Antibody Test

At day 2 after the onset, specific IgM antibody can be detected, with a titer of 1:20 being defined as positive; specific IgG antibody can also be detected positive with a titer of 1:40. An at least four times increase of the titer after 1 week has the diagnostic value.

Specific Antigen Test

For detection of the specific antigen, both immunofluorescence assay and ELISA are commonly applied while colloidal gold method shows more favorable sensitivity. In serum and peripheral blood of patients in the early stage of the disease, Hantavirus antigen can be detected from the neutrophils, monocytes, lymphocytes, and urinary sediment cells.

15.6.1.6 PCR

By RT-PCR, the RNA of HFRSV can be detected and the examination has a relatively high sensitivity, which facilitates the early diagnosis.

15.6.2 Diagnostic Imaging

15.6.2.1 X-Ray

X-ray is commonly applied for examining the thoracic and gastric lesions in patients with EHF.

15.6.2.2 Ultrasound

Ultrasound provides valuable data for abdominal parenchymal organ lesions in the patients with EHF.

15.6.2.3 CT Scanning

CT scanning has a larger range of detection than X-ray, which can be applied for examination of the whole body.

15.6.2.4 MR Imaging

MR imaging can demonstrate the radiological changes of the organs from multi-sections and multi-perspectives, which has special diagnostic significance for assessing various organ hemorrhage.

15.6.3 Other Examinations

15.6.3.1 Electrocardiography

EHF is demonstrated by electrocardiography with arrhythmia and myocardial lesions, such as sinus bradycardia and conduction block.

15.6.3.2 Intraocular Pressure and Fundus Examinations

Some patients experience increased intraocular pressure. An obviously increased intraocular pressure commonly predicts severe clinical conditions.

15.6.3.3 Renography

Since renal lesions are the most important pathological changes of EHF, renography at the early stage can demonstrate some apparent changes. Actually, renography demonstrates abnormalities during the whole course of the disease, mostly with bilateral acute obstructive lesions.

15.6.3.4 Gastroscopy

Gastroscopy can demonstrate diffuse congestion of the whole stomach, with scattering cord-like or grid-like hemorrhagic foci that are covered by blood scabs or fresh blood. Biopsy can also be performed for the examination.

15.7 Imaging Demonstrations

The imaging demonstrations of EHF can be quite different due to variance of onset and involved body system. Various radiological examinations are nonspecific to EHF but have clinical for some of its complications.

15.7.1 Central Nervous System

The central nervous system is mostly demonstrated with cerebral edema and cerebral hemorrhage. Hemorrhage may occur in brain parenchyma, subarachnoid space, or cerebral ventricle. EHF complicated by cerebral edema can occur in the febrile stage, hypotensive shock stage, oliguria stage, or its migrating period.

15.7.1.1 Cerebral Edema

CT scanning demonstrates cerebral edema as extensive symmetric density decrease in the cerebral white matter, which has a CT value of 12–25 Hu, unclearly defined interface between white and gray matters that extends into the subcortex. The lesions are mainly distributed in the bilateral frontal lobes, bilateral parietal lobes, and parieto-occipital junction, with narrowed or occlusive cerebral sulcus, fissures, and cistern as well as smaller cerebral ventricles (Fig. 15.1). MR imaging demonstrates long T1 long T2 signals. In cases with large area of cerebral edema, shift of brain midline structures can be demonstrated. In serious cases, cerebral herniation occurs.

Case Study 1

A male patient aged 25 years complained of fever, chills, headache, orbital pain, nausea, vomiting, and decreased volume of urination with no known causes for 4 days. He was then hospitalized. By physical examination, his body temperature was 38.5 °C and he had bulbar conjunctival congestion of both eyes, hemorrhagic spots in the skin of anterior chest, and bilateral renal percussive pain. By laboratory tests, WBC was 14.6×10^9/L, Scr was 621.5 μmol/L, and BUN was 13.6 mmol/L. At day 6 after hospitalization, he experienced sudden convulsion. And CT scanning defined the diagnosis of cerebral edema.

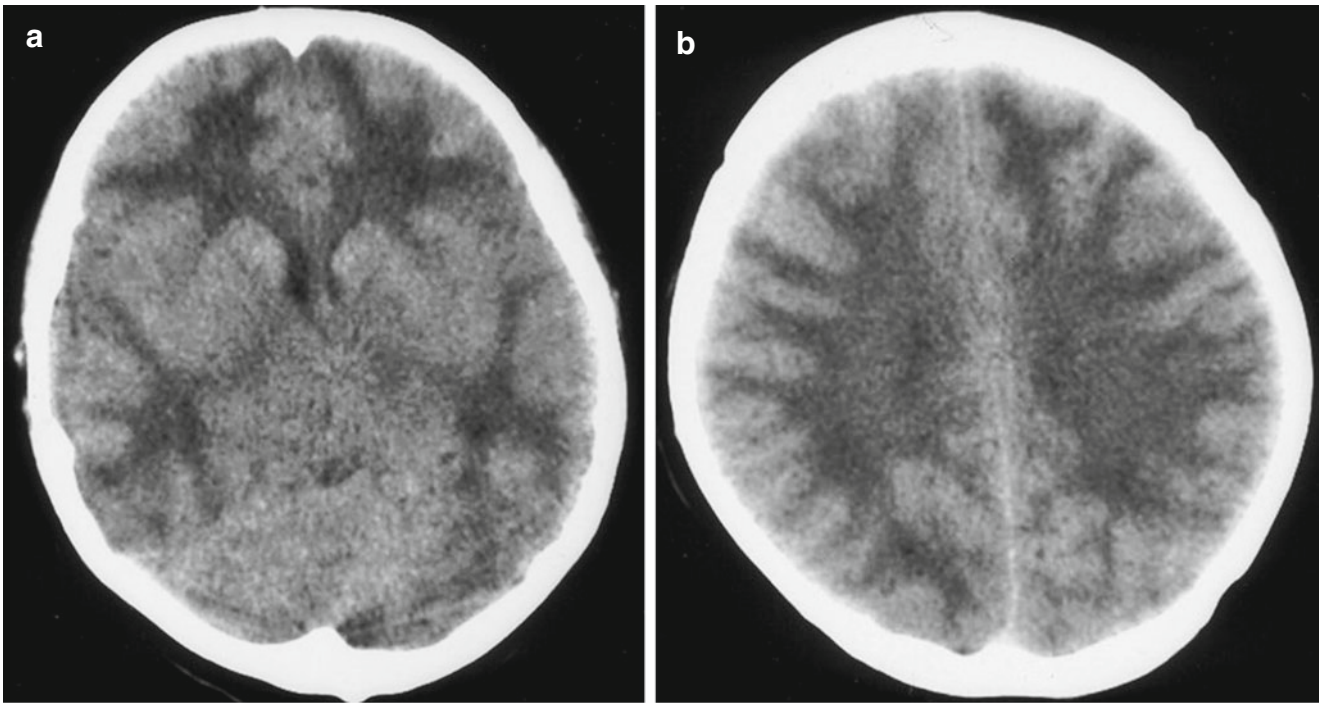

Fig. 15.1 EHF complicated by cerebral edema. (**a**, **b**) Plain CT scanning demonstrates symmetric density decrease in the cerebral white matter of cerebral hemispheres

15.7.1.2 Cerebral Hemorrhage

CT scanning is the examination of choice for the clinically suspected cases of EHF complicated by intracranial hemorrhage. Intracerebral hematoma is demonstrated by CT scanning as round- or oval-shaped evenly high-density lesion in the brain parenchyma with surrounding edema, well-defined boundary, and space-occupying effect (Fig. 15.2). Intracerebral hematoma is demonstrated by MR imaging as long T1 long T2 signals in the hyperacute stage, equal T1 short T2 signals in the acute stage, short T1 long T2 signals in the subacute stage, and long T1 long T2 signals in the chronic stage.

Case Study 2

A male patient aged 25 years complained of chills, fever, headache, lower back pain, orbital pain, nausea, vomiting, and decreased volume of urination with no known causes for 2 days. He was then hospitalized. By CT scanning, the diagnosis was defined to be intracerebral hemorrhage.

15.7.1.3 Subarachnoid Space Hemorrhage

CT scanning is the examination of choice for the diagnosis of subarachnoid space hemorrhage, which is demonstrated as increased density in the cerebral sulcus, fissures, and cistern (Fig. 15.3). MR imaging tends to misdiagnose acute subarachnoid space hemorrhage. T1WI demonstrates high signals in cases of subacute subarachnoid space hemorrhage, while T2WI demonstrates low signals in cases of chronic subarachnoid space hemorrhage.

Case Study 3

A male patient aged 22 years complained of aversion to cold, fever, and oliguria for 8 days with accompanying headache, lower back pain, orbital pain, nausea, and vomiting. After he was hospitalized, by physical examination, his body temperature was 39.6 °C and he had drunken-like appearance, bulbar conjunctival congestion of both eyes, subaxillary hemorrhagic spots, and bilateral renal percussive pain. At day 4 after the hospitalization, he experienced convulsion and meningeal irritation sign. By laboratory tests, WBC was 12.4×10^9/L, Scr was 450 μmol/L, and BUN was 32.7 mmol/L. By CT scanning at day 5, the diagnosis was defined as subarachnoid space hemorrhage.

15.7.2 Respiratory System

15.7.2.1 Lung Congestion

Pulmonary congestion mainly occurs in the febrile stage. X-ray demonstrates enlarged hilar shadow; thickened, increased, and deranged lung markings; as well as excessively

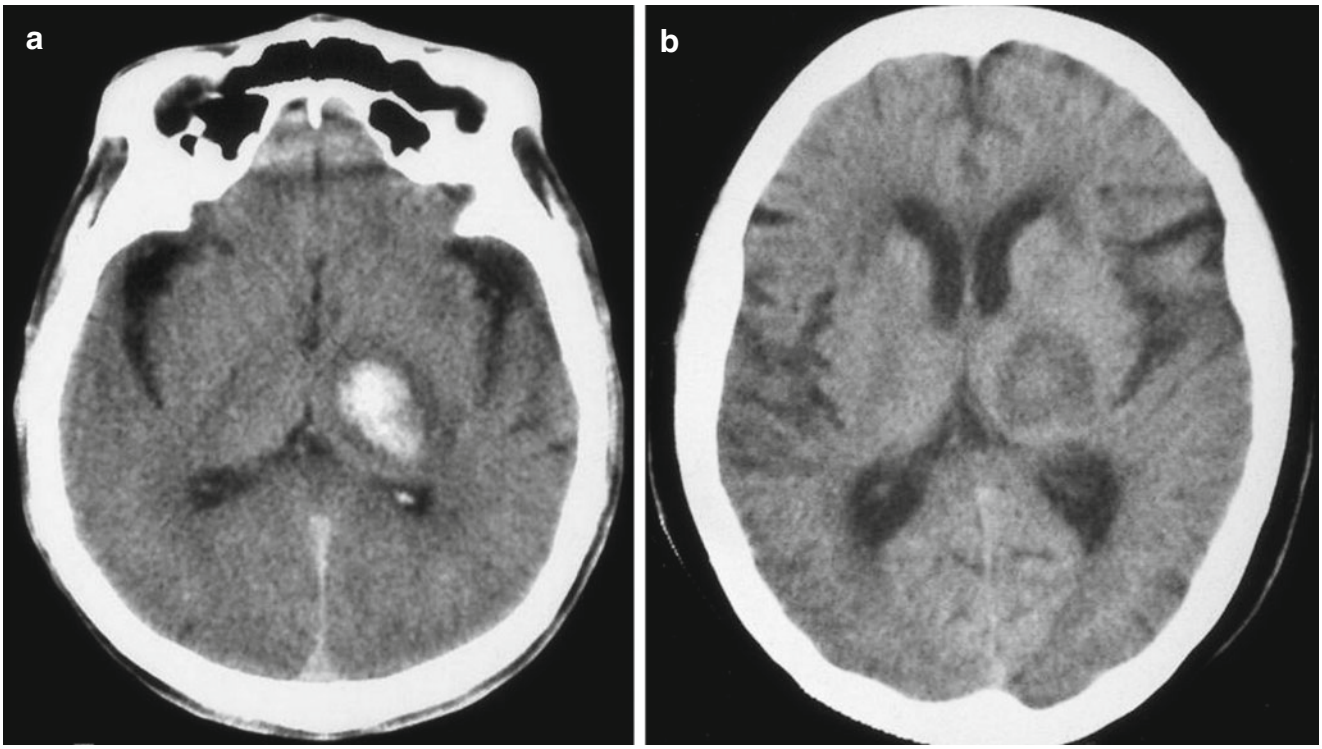

Fig. 15.2 EHF complicated by cerebral hemorrhage. (**a**) Plain CT scanning demonstrates hemorrhage in the left thalamus and peripheral edema. (**b**) Reexamination by CT scanning after 20 days demonstrates absorption of hematoma

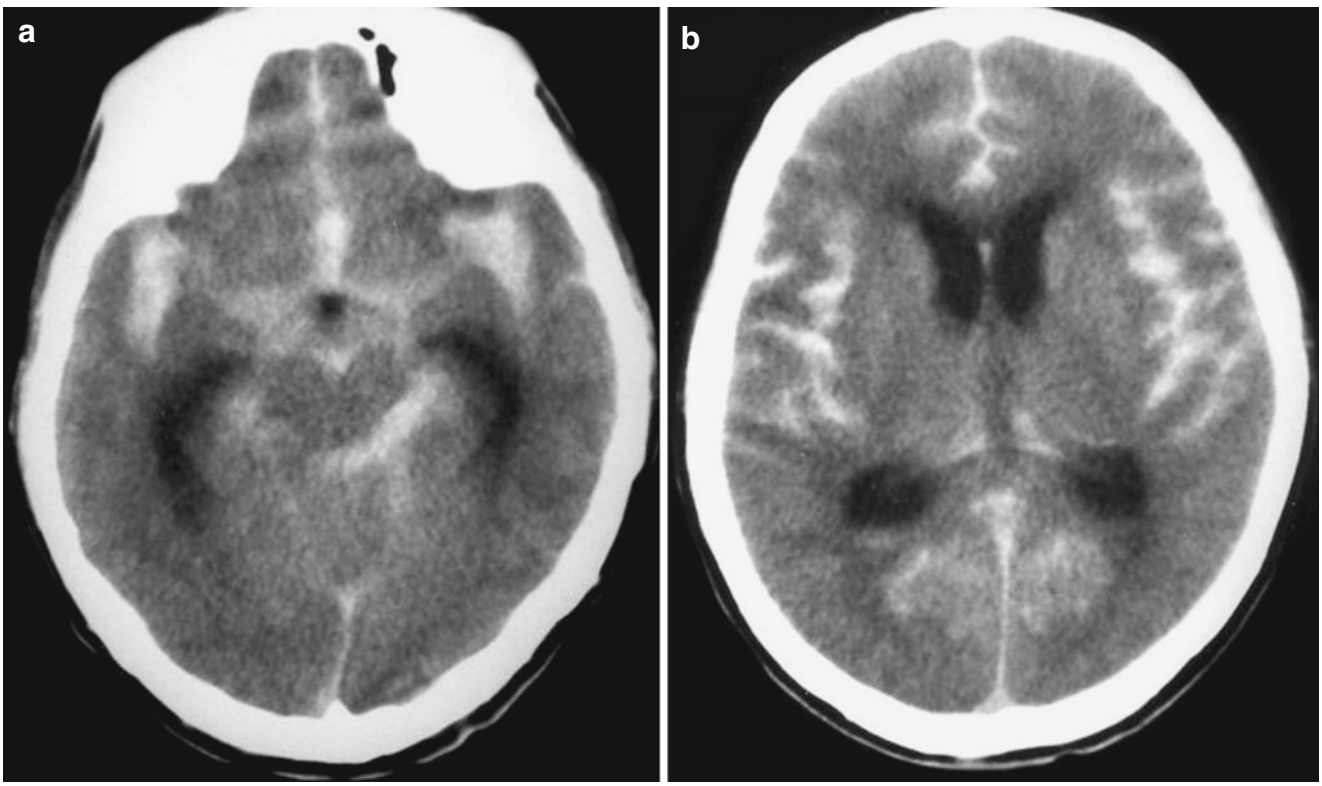

Fig. 15.3 EHF complicated by subarachnoid space hemorrhage. (**a**, **b**) Plain CT scanning demonstrates high-density hemorrhagic foci in the suprasellar cistern, lateral fissure cistern, ambient cistern, and cerebral sulcus

decreased transparency of the lung field. CT scanning demonstrates enlarged hilum in both lungs, thickened and twisted pulmonary arterial branch, and ground-glass opacity of the lung field. In addition, rare patients are demonstrated with pleural thickening.

15.7.2.2 Pulmonary Edema

Interstitial pulmonary edema mainly occurs in the terminal febrile stage and the hypotensive shock stage. X-ray demonstrates enlarged hilar shadow, thickened and blurry pulmonary vascular branches, excessively decreased transparency of the lung field, and spots or flakes of ground-glass shadows distributed unevenly and asymmetrically in both lungs. There are also nodular cuff sign, reticular shadow, interlobular septal line and cord-like shadows, enlarged heart shadow, as well as blunt costophrenic angle. In cases with aggravated pulmonary vascular lesions, pulmonary alveolar edema can be found mainly in the hypotensive shock or oliguria stage. X-ray demonstrates enlarged intrapulmonary shadows distributed symmetrically with the hilum as the center, which extend into the lung field of both lungs with decreased coloring and excessively decreased transparency of lung fields (Fig. 15.4). Otherwise, X-ray demonstrates large or small flakes of intrapulmonary shadows confined in only one pulmonary lobe with poorly defined boundary, possibly demonstration of enlarged heart shadow, and increased cardiothoracic ratio. In cases with pericardial effusion, flask-shaped heart shadow is demonstrated while pleural reactions are demonstrated as blunt costophrenic angle. CT scanning clearly demonstrates a small quantity of pleural effusion, pleural thickening, and pericardial effusion as pericardial thickening and liquid density shadow in the pericardium (Fig. 15.5).

Case Study 4

A male patient aged 46 years complained of fever for 7 days and oliguria for 3 days. He reported a history of contact to rats during field construction work. He experienced typically drunken-like appearance and pinpoint-like hemorrhagic spots in his right armpit. After receiving the therapies for anti-infection, hemostasis, and diuresis for 5 days, his body temperature returned to normal and the volume of urination also returned to normal. By routine urine test, protein was positive (+) and granular cast was also positive (+++). By electrocardiography, no abnormalities were found. By X-ray, there was pulmonary edema. And 7 days later, the disease is completely cured with no lesions detected.

Case Study 5

A male patient aged 32 years complained of fever, cough, and lower back pain for 2 days and was hospitalized. He experienced typically drunken-like appearance and pinpoint-like hemorrhagic spots in the skin of the chest. By physical examination, his body temperature was 39.8 °C. By laboratory tests, urine volume was 1500 ml per 24 h that reaches 6200 ml per 24 h after 5 days, urine protein was positive (++), granular casts were positive, and blood BUN was 10.8 mmol/L.

15.7.2.3 Pulmonary Infection

Pulmonary infection may occur in any stage of EHF, but mostly in oliguria stage and diuresis stage. X-ray and CT scanning demonstrate patches of blurry shadows diffusely distributed along singular or bilateral lung markings. In rare cases, small patches of increased-density shadows are demonstrated, possibly with decreased transparency of both lower lungs and quite even distribution. Their fusion into large flakes can be locally found (Figs. 15.6 and 15.7).

Case Study 6

A female patient aged 24 years complained of aversion to cold, fever, lower back pain, orbital pain, nausea, vomiting, and decreased volume of urination with no known causes for 3 days and she was then hospitalized.

Case Study 7

A male patient aged 52 years was admitted to the hospital due to the complaints of fever, cough, and chest pain for 4 days. He experienced typically drunken-like appearance and pinpoint-like hemorrhagic spots in the skin of the chest. By physical examination, his body temperature was 39.2 °C, and he had drumlike sounds in bilateral thoracic cavity by auscultation. By laboratory tests, the volume of urination was 1250 ml that reached 4300 ml after 5 days, urine protein was positive, granular casts were positive, and BUN was 10.2 mmol/L.

15.7.2.4 Pulmonary Hemorrhage

X-ray and CT scanning demonstrate diffusely distributed intrapulmonary consolidation shadows with ground-glass density or large flakes of high density (Fig. 15.8).

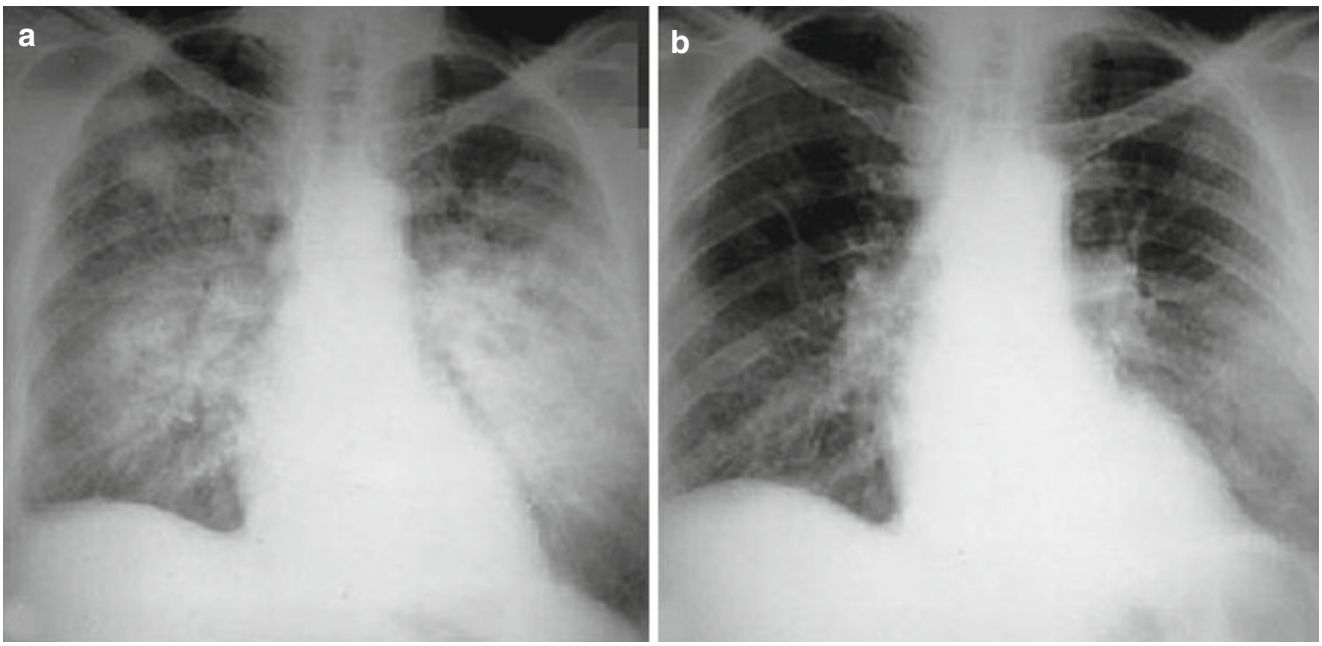

Fig. 15.4 EHF complicated by pulmonary edema. (**a**) X-ray demonstrates symmetrically enlarged hilum of both lungs and large flakes of light and thin cloudy shadows in the medial part of both lower lungs. (**b**) Reexamination after 7 days demonstrates absorption of most lesions

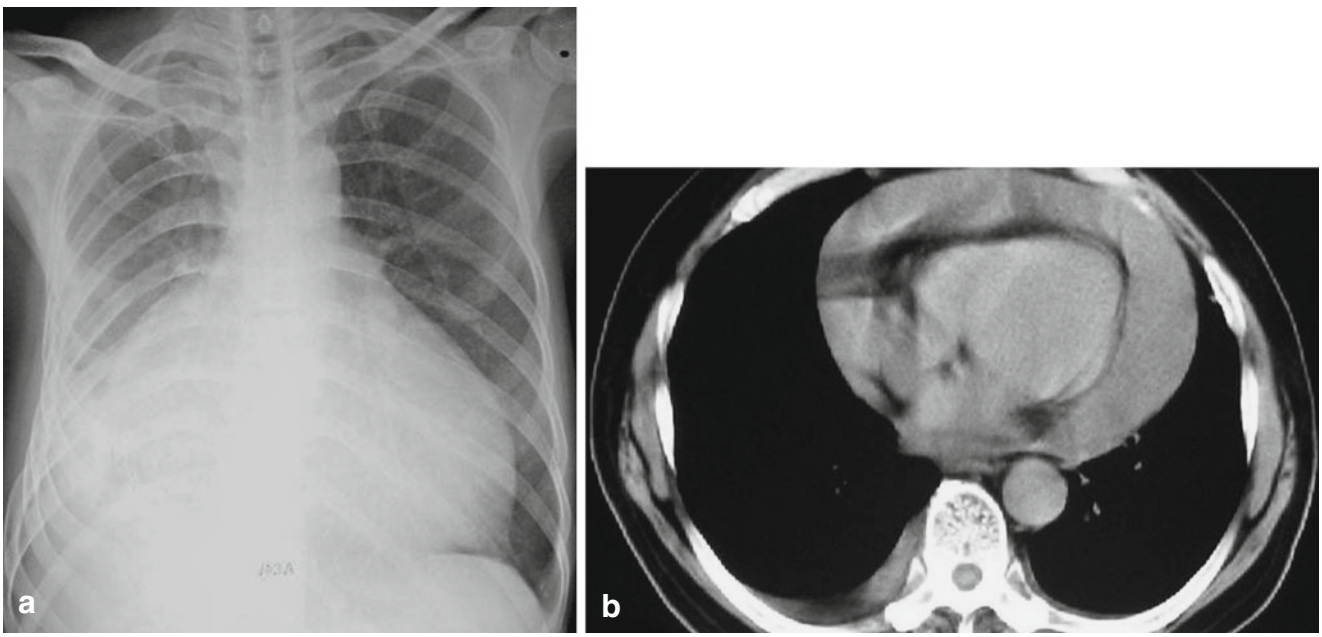

Fig. 15.5 EHF complicated by pericardial and pleural effusion. (**a**) X-ray demonstrates enlarged heart shadow in flask-like shape as well as absent right diaphragmatic surface and costophrenic angle. (**b**) CT scanning demonstrates arch-shaped low-density shadow in the right thoracic cavity as well as pericardial thickening with liquid-like low density

Case Study 8

A male patient aged 45 years complained of fever, headache, and lower back pain for 7 days as well as oliguria for 2 days. After hospitalization, he experienced persistent fever with the highest body temperature of 40 °C, systemic soreness and pain, severe headache, orbital pain, lower back pain, and accompanying cough with bloody sputum.

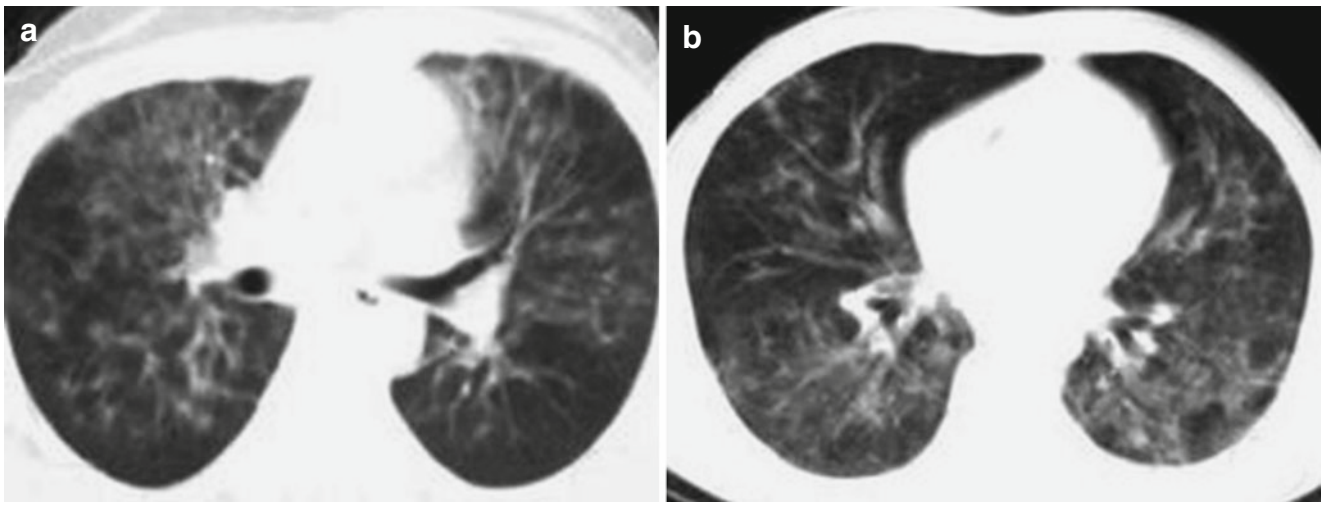

Fig. 15.6 EHF complicated by double pneumonia. (**a**, **b**) CT scanning demonstrates multiple small flakes of ground-glass shadows in both lungs

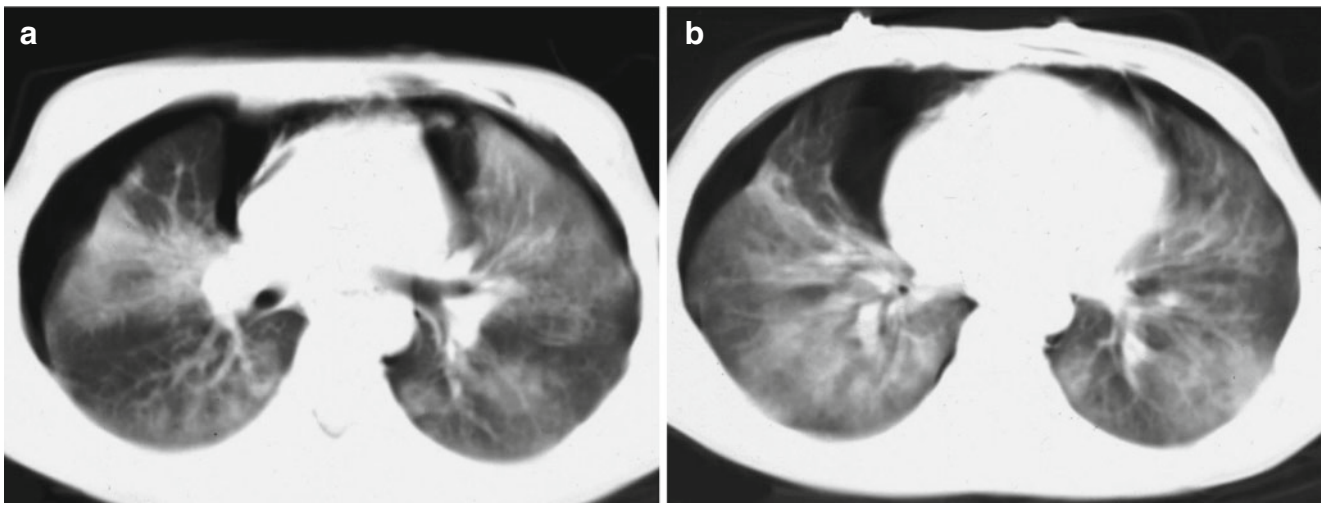

Fig. 15.7 EHF complicated by double pneumonia and double pneumothorax. (**a**, **b**) Plain CT scanning demonstrates large flakes and patches of shadows with poorly defined boundaries in both lungs as well as pulmonary area with no lung marking in the lateral part of lung fields in bilateral thoracic cavity

15.7.3 Digestive System

15.7.3.1 Hepatic and Splenic Changes

Both liver and spleen are the target organs of hemorrhagic fever virus, and the patients with EHF experience different degrees of hepatic and splenic lesions. Ultrasound demonstrates enlarged liver, increased echo from the liver parenchyma, as well as dense, increased, and enhanced light spots. CT scanning demonstrates enlarged and plump liver, diffusively decreased density of the liver parenchyma whose CT value being lower than the spleen, and poorly defined intrahepatic ducts. In cases with complication of intrahepatic hematoma, intrahepatic high-density hemorrhagic lesions can be found, with formation of liquid level and enlarged spleen.

15.7.3.2 Pancreatic Changes

EHF complicated by acute pancreatitis rarely occurs. Pancreatic swelling is commonly caused by pancreatic vascular dilation, congestion, edema, and hemorrhage or occlusive pancreatic duct-induced juice retention due to swelling or compressed epithelial cells of the pancreatic ducts or pancreatic tissues. Pancreas ultrasound demonstrates swollen and enlarged pancreas with enhanced echo from the parenchyma. CT scanning demonstrates swollen and enlarged pancreas with poorly defined boundary. In some serious cases, peripancreatic hematoma can be demonstrated, with increased density in the perirenal fascia and intestinal mesentery. In cases complicated by intrapancreatic hematoma, the lesions are demonstrated with high-density fluid level.

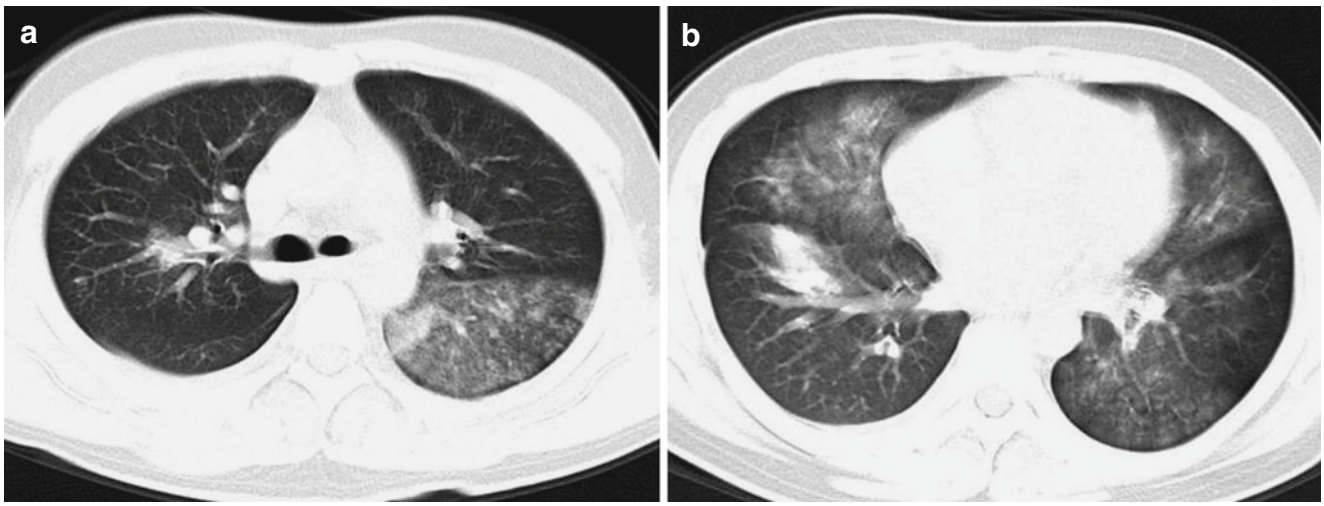

Fig. 15.8 EHF complicated by pulmonary hemorrhage. (**a**, **b**) Plain CT scanning demonstrates patches of shadows with ground-glass-like density in both lungs with poorly defined boundaries

15.7.3.3 Gallbladder Changes

Coarse and thickened gallbladder is commonly caused by hepatic lesions and hypoproteinemia, which commonly coexist with hydrothorax and ascites. Both ultrasound and CT scanning demonstrate irregular thickening of gallbladder wall, even echoes or density in the gallbladder, as well as gallbladder fossa effusion.

15.7.3.4 Gastrointestinal Changes

Gastrointestinal barium meal X-ray demonstrates erosive lesions in the gastric mucosa, linear superficial ulceration, as well as thick and twisted gastric mucosa that is especially obvious in the mucosa of gastric fundus and body. But the more serious lesions are found in the mucosa of the anteroposterior wall of greater curvature.

CT scanning demonstrates even thickening of the gastrointestinal wall with decreased density. In cases with hemorrhage in the gastrointestinal mucosa, the density can be demonstrated with uneven increase and the density of intestinal mesentery can be demonstrated with uneven increase. Some patients may also experience incomplete intestinal obstruction such as intestinal canal dilation and inflation.

15.7.3.5 Abdominal and Retroperitoneal Changes

The main pathological findings are ascites and retroperitoneal hematoma. Ascites is mostly found in the febrile stage, hypotensive shock stage, and oliguria stage, with the highest incidence rare during the hypotensive shock and oliguria stages. The earliest occurrence of ascites is usually within the first 3 days of the whole illness course. Ultrasound demonstrates liquid echo from the abdominal cavity. CT scanning demonstrates small quantities of liquid in the liver periphery, spleen periphery, and gallbladder fossa whose CT value is higher than leakage fluid. In cases complicated by peritoneal hemorrhage or retroperitoneal hematoma, ultrasound demonstrates retroperitoneal high echo. For cases with hemorrhage of fresh blood, wave at liquid level segment can be demonstrated. CT scanning demonstrates diffusely increased density in the retroperitoneal adipose layer and abdominal or retroperitoneal hematoma as mass-like or nodular uneven high-density shadows. For cases with old hematoma, equally high or equally low mixed-density shadows are demonstrated.

15.7.4 Urinary System

Based on the staging of EHF, the renal lesions at different stages have different radiological demonstrations. In the febrile stage, both kidneys are demonstrated with normal morphology or slightly symmetric enlargement and no obvious morphological changes in the renal calices and renal pelvic cavity. In the hypotensive shock stage, the kidneys are demonstrated to be swollen like a ball, smaller space of renal pelvic cavity, and poorly defined renal calices. In the oliguria stage, the kidneys are demonstrated with obvious symmetric enlargement in sphere shape, aggregated kidney calices, smaller volume of the spaces in renal pelvic cavity, and the density ratio of renal cortex to medulla being less than 1. In the diuresis stage, the kidneys are demonstrated with normal morphology and size, which is almost the same as the normal kidneys. During the initial stage after onset, renography demonstrates obvious changes, indicating obvious renal insufficiency at the early stage of the disease.

15.7.4.1 Ultrasound

Ultrasound is the simplest and feasible examination for detection of renal lesions, which favorably demonstrates renal swelling, edema, congestion, and hemorrhage, which

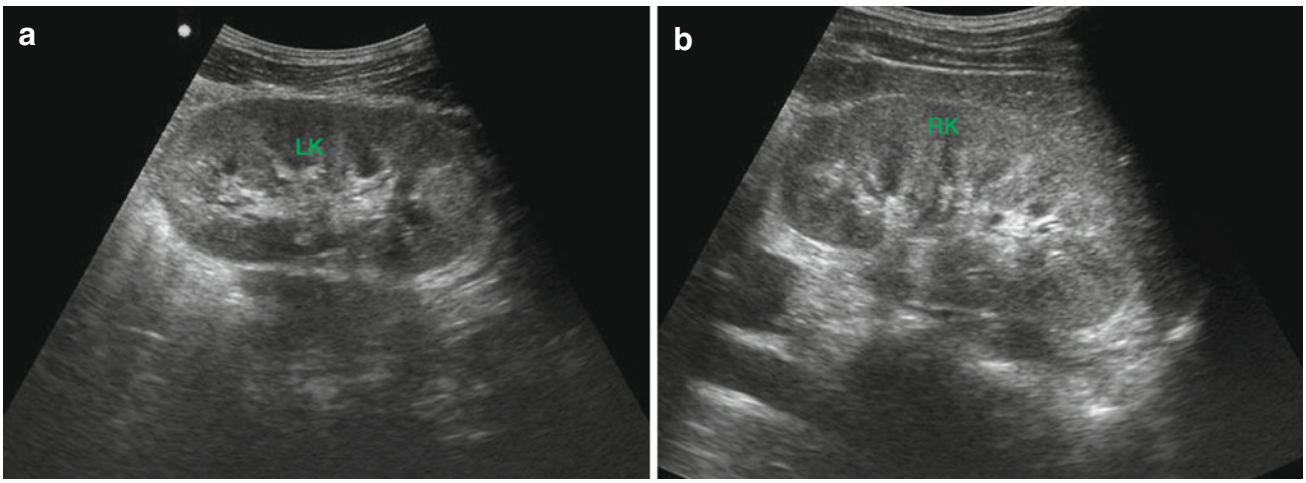

Fig. 15.9 EHF complicated by renal lesions. (**a**, **b**) Color Doppler ultrasound demonstrates enlarged volume of both kidneys with well-defined contour, strengthened echo from the renal parenchyma, well-defined interface between renal cortex and medulla, and quite well-arranged renal sinuses

are characteristic. Specifically, both kidneys are subject to symmetric enlargement that is more obvious in the anteroposterior diameter. Several oval-shaped no-echo areas are demonstrated with similar size and shape in the obviously thickened renal parenchyma that surrounds and deforms the collecting system due to compression. Irregular liquid dark area is demonstrated between the renal columns of both kidneys, with obviously decreased and scattering echoes from the renal sinus. The structures of renal cortex and medulla are deranged and blurry and dark echo areas are demonstrated under the renal capsule or in the renal adipose cyst, which are caused by hemorrhage. Mixed echoes with different intensities are demonstrated in the perinephral space (Fig. 15.9).

Case Study 9

A male patient aged 18 years experienced fever, headache, pharyngalgia, and systemic pain of the whole body. He was admitted to the hospital due to diagnosis of upper respiratory tract infection. By laboratory tests, there was increased WBC and decreased thrombocytes. By routine urine test, RBC was positive (+++), urine protein was positive (++), and BUN was increased.

Color Doppler flow imaging (CDFI) demonstrates basically normal blood flow in the kidneys in the febrile stage, obviously less blood flow signals in the kidneys in the oliguria stage, low flow speed due to high resistance, and obviously increased resistance index. In the convalescence stage, it is demonstrated with gradually more blood flow signals till recovery. Based on renographical changes, the severity of the conditions can be assessed and the prognosis can be predicted. When the conditions improved, the volume of the kidney is gradually smaller, with normal thicknesses of the renal parenchyma and renal sinus, and low echo from the cortex, which are indicators for assessment of therapeutic efficacy.

15.7.4.2 CT Scanning

CT scanning demonstrates swollen kidneys that are commonly bilaterally symmetric enlargement with more obvious enlargement of the anteroposterior diameter. In addition, there are thickened renal parenchyma, possibly uneven density of the renal parenchyma, low density of renal cortex, relatively high density of renal medulla, small renal sinuses, and poorly defined renal calices. The more above abnormalities indicate more reliable evidence supporting renal enlargement (Fig. 15.10). In those EHF cases with no renal enlargement, each of the above demonstrations can be found alone. Perinephric and paranephric spaces are absent. Perinephric edema and effusion cause increased density of adipose. Renal rupture and hemorrhage are demonstrated as intranephric hematoma, which is mass-like high-density shadow by CT scanning and no enhancement of the lesion by contrast scanning. Subcapsular hematoma is caused by blood retention in the renal capsule, with demonstrations of half-moon-like abnormal density in the lateral margin of the kidney. In cases with fresh hemorrhage, high density is demonstrated, with a CT value above 60 Hu. By follow-up examination, the density of hematoma is demonstrated with gradual decrease to low level (Figs. 15.11 and 15.12). Perinephric exudation is demonstrated as perinephric effusion, with thickened perinephric fascia, and mixed-density cord-like shadows in the paranephric space.

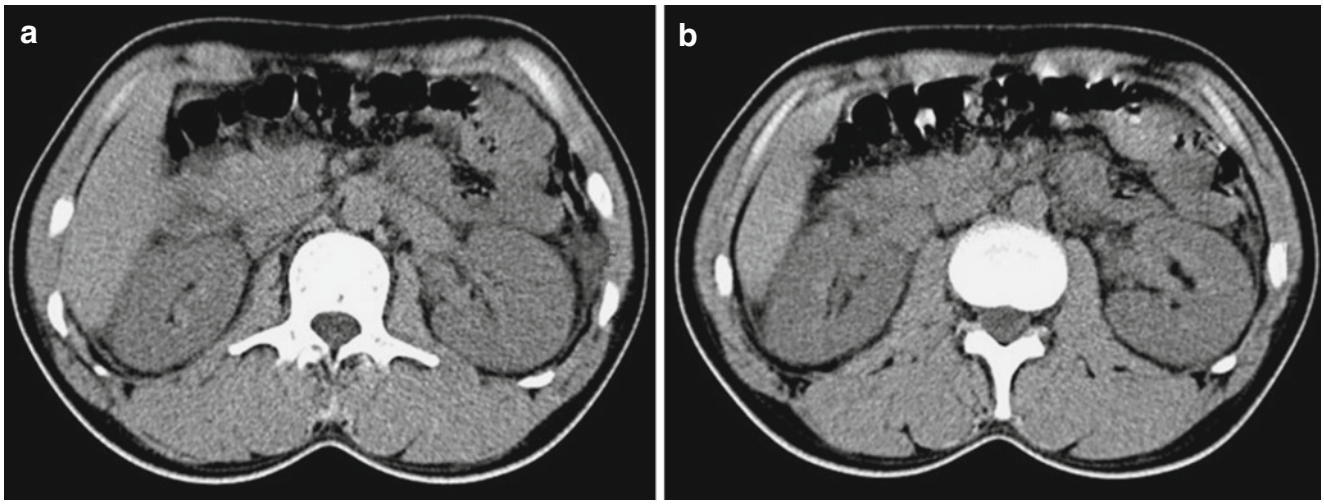

Fig. 15.10 EHF complicated by bilateral renal enlargement. (**a**, **b**) Plain CT scanning demonstrates enlarged volume of both kidneys with poorly defined boundaries

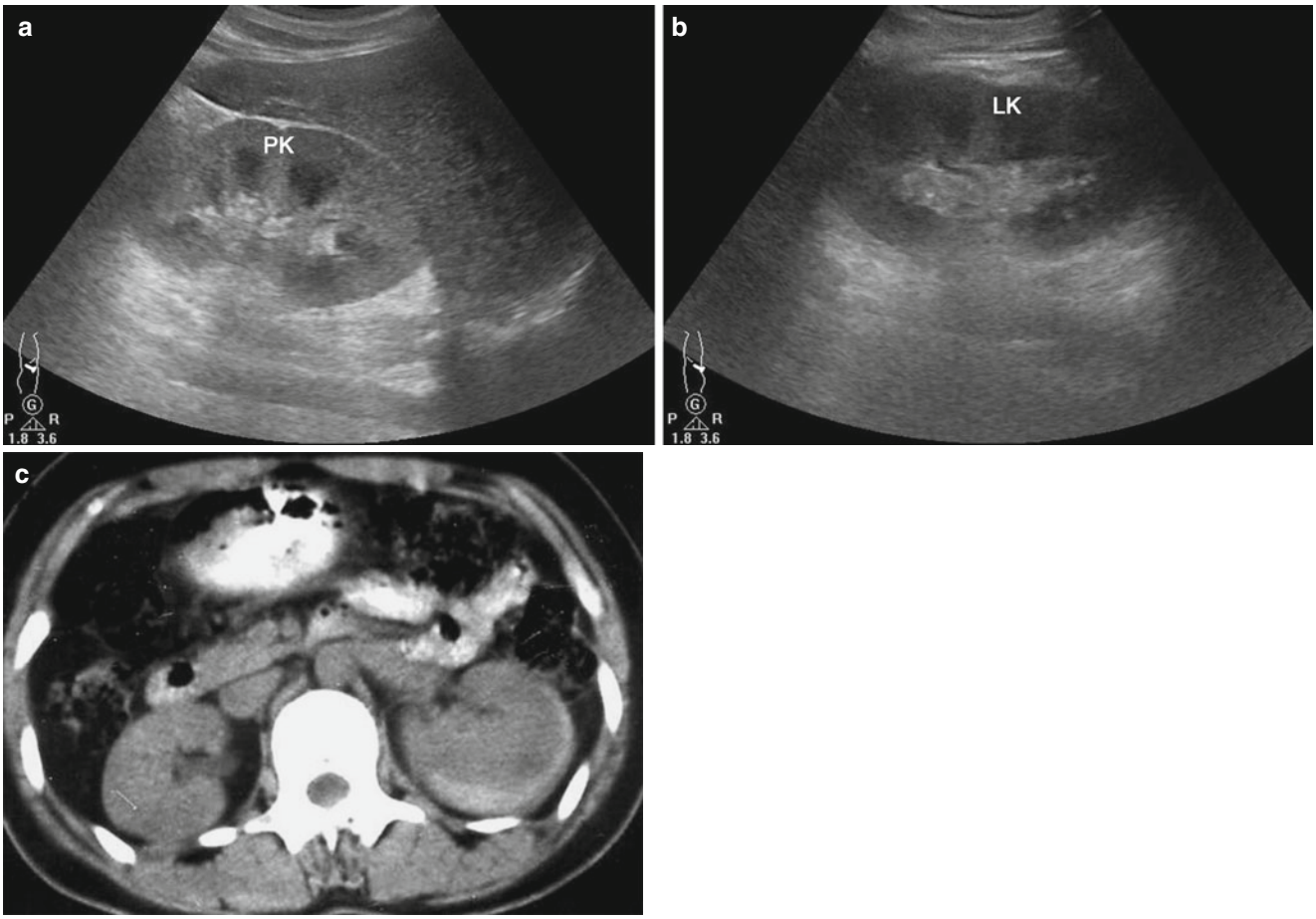

Fig. 15.11 EHF complicated by bilateral renal enlargement and left renal hematoma. (**a**, **b**) Ultrasound demonstrates enlarged and plump kidneys, with enhanced echoes from parenchyma, well-defined interface between renal cortex and medulla, and well-arranged renal sinuses. Around the left kidney, dark area with low echo is demonstrated. (**c**) Plain CT scanning demonstrates crescent-shaped high-density shadow under the capsule of left kidney, obviously thickened parenchyma of the left kidney, and smaller renal pelvis

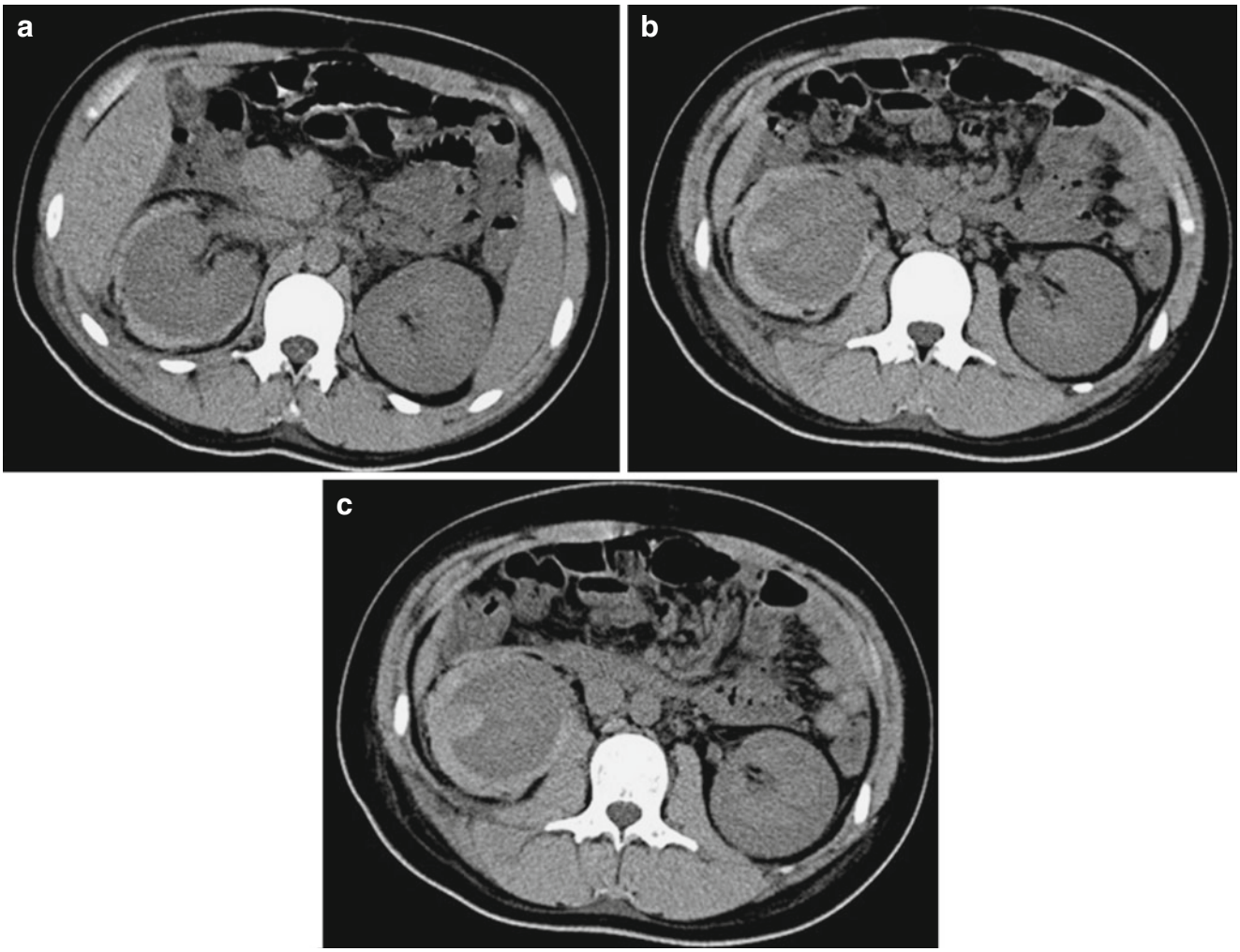

Fig. 15.12 EHF complicated by bilateral renal enlargement and right kidney hemorrhage. (**a**–**c**) Plain CT scanning demonstrates enlarged volume of both kidneys, obviously thickened renal parenchyma, decreased size of renal pelvis, round-like high-density shadows in the right renal parenchyma, and crescent-shaped high-density shadows under the right kidney capsule. (Note: Cases 10 and 12 as well as the figures were provided by Wu JP and Yun J from *The 3rd People's Hospital, Changzhou, Jiangsu, China*)

Case Study 10

A male patient aged 38 years complained of fever, headache and lower back pain for 4 days, and oliguria for 2 days and he was hospitalized. By laboratory tests, WBC was 2.84×10^9/L, PTL was 84×10^9/L, urine protein was positive (++), and EHF IgG antibody and EHF IgM antibody were positive.

Case Study 11

A male patient aged 44 years was hospitalized due to fever, systemic soreness and pain of the whole body, nausea, abdominal pain, and diarrhea. By physical examination, his abdomen was soft with mild tenderness, he had no enlargement of the liver and spleen, and he had percussive pain in both kidneys. By laboratory tests, WBC was increased, PTL was decreased, urine erythrocytes was positive (+++), urine protein was positive (++), and BUN was increased.

Case Study 12

A boy aged 13 years complained of fever, headache, and lower back soreness for 4 days. After the hospitalization, the laboratory tests demonstrated WBC 18.3×10^9/L and PTL 40×10^9/L.

Contrast CT scanning demonstrates weakened renal enhancement and prolonged time in the poorly defined interface between renal cortex and medulla. In the patients with severe renal dysfunctions, contrast CT scanning should not be ordered. The low density demonstrated in the renal cortex by contrast CT scanning is possibly induced by abnormal perfusion of the renal cortex. The enhancements of renal parenchyma are not distributed in renal segments, with adjacent renal segments extending to each other to the renal sheath. It is believed that the prolonged time for enhancement of renal parenchyma by CT scanning is corresponding to prolonged time for kidney imaging during intravenous pyelography.

15.7.4.3 Renography

Since renal lesions are the most important pathological changes caused by EHF, renography can immediately demonstrate some apparent changes in the early stage of the disease. Actually, renography demonstrates abnormalities during the whole course of the disease, most of which are bilateral acute obstructive changes (Fig. 15.13). In the febrile stage of EHF, renography demonstrates some mild changes, with decreased peak value and slightly prolonged half discharge time, indicating renal tubular mild lesions at the early stage of EHF. In the oliguria stage, renography demonstrates low-level extending line with no ascending section and excretive section, indicating severe renal tubular dysfunctions. In the diuresis stage, renography demonstrates asymmetrical parabolic curve with slow ascending and descending segments as well as low peak value, indicating partial recovery of renal tubular functions. Meanwhile, the renal glomerular functions are normal. Such glomerulotubular functional unbalance causes frequent urination with increased volume. In the convalescent stage, renography demonstrates low peak value and delayed excretion. From the above renographic demonstrations, we know that renal tubular lesions exist in the whole course of EHF.

Case Study 13

A male patient aged 47 years complained of fever and headache for 3 days, with percussion pain in the kidneys. By physical examination, he had drunken-like appearance, bulbar conjunctival congestion, dense hemorrhagic spots in the groin, and scattering hemorrhagic spots in the left chest wall, back, and the lower 1/3 part of left anteromedial forearm. CT scanning demonstrated no abnormalities at the early and convalescence stages, while enlarged kidneys and perinephric exudation of both kidneys at the middle stage. Renography demonstrated bilaterally acute obstructive lesions in the left kidney, right kidney, and precardial area.

15.8 Diagnostic Basis

15.8.1 Clinical Diagnosis

15.8.1.1 Epidemiological Data

In the epidemic seasons of EHF, some patients have a history of visiting the epidemic area or natural epidemic focus within 2 months prior to the onset. In some other cases, the patients may work or live in the epidemic area for years. Still in some other cases, the patients have a history of direct or indirect contact to rats or mice. Otherwise, the patients have a history of intake of contaminated food by rats or have a history of contact to experimental animals carrying the viruses.

15.8.1.2 Clinical Manifestations

The disease has an acute onset and the patients experience fever; triple pain of headache, orbital pain, and low back pain; nausea; vomiting; abdominal pain; and diarrhea. The patients commonly experience successive hypotension, oliguria, and diuresis. The skin is subject to triple redness, and in some serious cases, the patients may even show drunken-like appearance. The mucosa is subject to triple redness. Hemorrhagic spots are found in the armpit and anterior chest, with accompanying conjunctival edema, eyelid edema, facial edema, and renal percussive pain.

15.8.1.3 Laboratory Tests

Routine Blood Test

By routine blood test, there are increased erythrocytes and hemoglobin, increased WBC count, decreased PLT, a large quantity of urine protein, and urine with membranous substance, all of which facilitate the diagnosis.

Serological Test

Double sera are detected for HV antibodies. The titer with an at least four times increase is defined positive. The paired sera test demonstrates at least four times increase of the titer of serum-specific IgG antibody can define the diagnosis.

15.8.1.4 Clinical Course

EHF patients should show the three major signs: fever, hemorrhage, and renal lesions. The whole course of disease includes febrile stage, hypotensive shock stage, oliguria stage, diuresis stage, and convalescence stage. Atypical cases or some cases with appropriate early treatment do not undergo hypotensive shock stage or oliguria stage but mostly still experience febrile and diuresis stages. Some severe patients may experience overlapping of two or three stages.

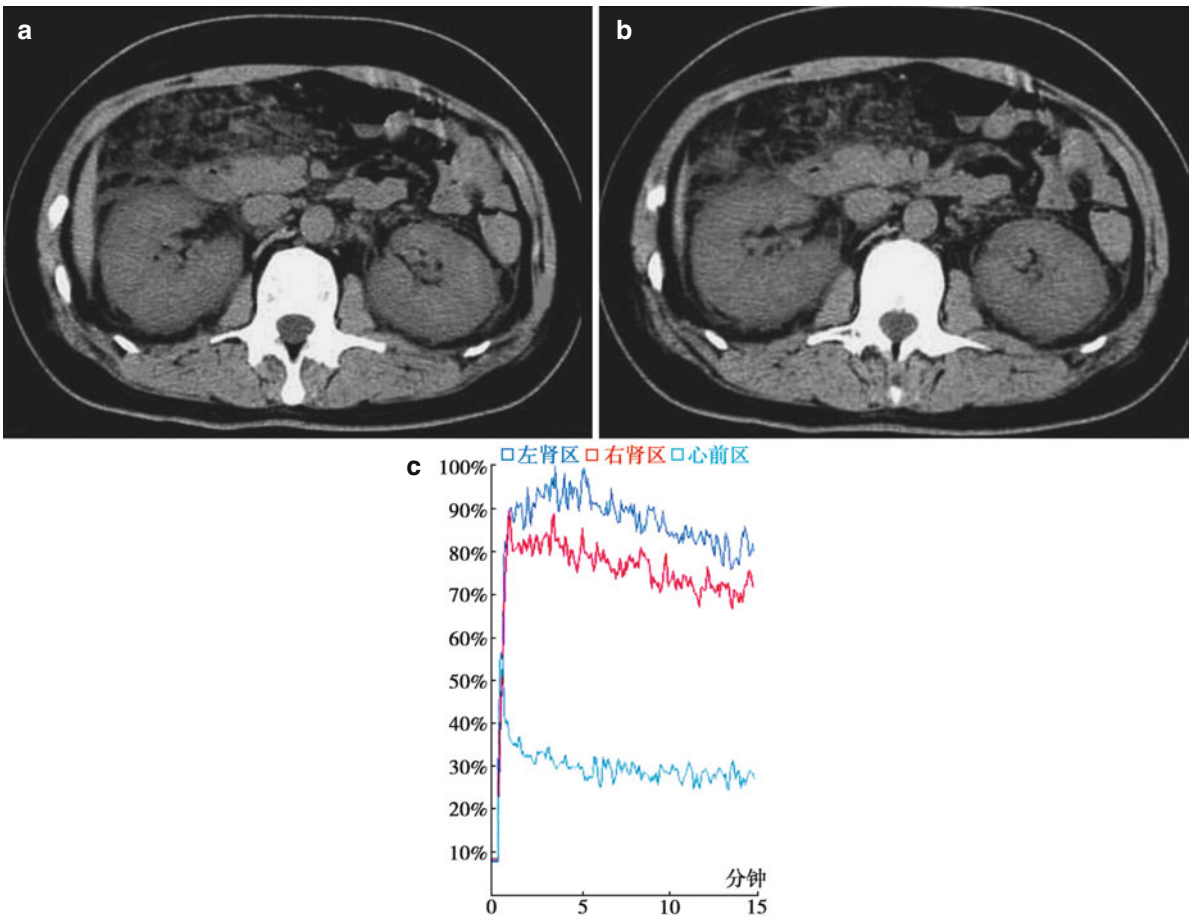

Fig. 15.13 EHF complicated by renal lesions. (**a**, **b**) Plain CT scanning demonstrates enlarged kidneys that are more obvious in the right kidney and rough perinephric fascia with increased density. (**c**) In the febrile stage, renography demonstrates decreased peak value and slightly prolonged half discharge time of the kidney

15.8.2 Diagnostic Imaging

The radiological demonstrations of EHF can be quite different due to the different onset time and different systems involved. The main demonstrations are as follows.

15.8.2.1 Central Nervous System

Radiology of the central nervous system demonstrates cerebral edema and cerebral hemorrhage.

15.8.2.2 Chest

Radiological examinations of chest demonstrate pulmonary edema, pulmonary infection, pulmonary hemorrhage, pleural effusion, and pericardial effusion.

15.8.2.3 Abdomen

Radiological examination of abdomen demonstrates different lesions due to variant stage and the organs involved. The lesions include hepatosplenomegaly, pancreatitis, cholecystitis, ascites, and retroperitoneal hematoma.

15.8.2.4 Kidney

Radiological examinations of kidney demonstrate different lesions due to variant stage, mainly including renal enlargement and abnormal renal density.

15.9 Differential Diagnosis

Due to the complex conditions of EHF, the clinical manifestations are special and the disease develops rapidly. Therefore, it tends to be misdiagnosed as other diseases. Therefore, the differential diagnosis is especially important. In Table 15.1, we list some key points for its differential diagnosis.

15.9.1 Influenza, Viral Upper Respiratory Tract Infection, and Common Cold

The patients with influenza, viral upper respiratory tract infection, or common cold experience extremely similar symptoms

Table 15.1 Differential diagnosis of EHF

Disease	Epidemiologic	Clinical	Laboratory	Radiological
EHF	Sporadic, during winter and springs from Oct. to Feb.	Fever, hemorrhage, renal lesions, triple pain, skin triple redness, mucosa triple redness	Variant at different stage, with obvious urine protein and renal insufficiency	Renal lesions and organ hemorrhage
Influenza, viral upper respiratory tract infection, and common cold	Simultaneous occurrence in a group of people in winters and springs	Respiratory tract catarrhal symptoms, skin hemorrhagic spots in the trunk	Relatively low WBC count	No obvious changes; typical patches of consolidation in the lungs
Leptospirosis	Highly sporadic, history of contact to contaminated water, in rainy seasons like summers and autumns and early winters	Systemic pain and weakness, obvious tenderness in the gastrocnemius, enlarged lymph nodes, hemorrhagic spots in the trunk and limbs	Increased WBC count, possibly urine protein and renal dysfunction, responsive to penicillin treatment	Pulmonary interstitial changes, intrapulmonary miliary nodules and pneumonia, enlarged heart shadow and pleural thickening
Typhoid fever	Summers and autumns	Reluctant complexion, tinnitus, double hearing, intestinal hemorrhage, and perforation	Decreased WBC count, normal PLT, blood and bone marrow cultures positive	Hepatosplenomegaly, thickened ileocecal wall, enlarged mesenteric lymph nodes, cholecystitis, enlarged appendix
Gastroenteritis and acute bacillary dysentery	Summers and autumns, a history of excessive eating and drinking or unhygienic food intake	Gastrointestinal symptoms, mild systemic symptoms	Routine stool test abnormal	By gastrointestinal X-ray, dilated intestine, rapid peristalsis, intragastric fluid retention
Acute abdomen	No certain seasonal prevalence	Acute abdominal pain, fever, obvious abdominal tenderness and rebound tenderness, tense abdominal muscle	Increased WBC count, a small quantity of urine protein	Dilation and pneumatosis of intestinal canal, thickened intestinal wall, free gas in abdominal cavity, ascites, acute cholecystitis and pancreatitis
Pulmonary infection	No certain seasonal prevalence	Fever, respiratory symptoms, pulmonary signs	Increased WBC count	Intrapulmonary consolidation, pleural effusion
Septicemia	No certain seasonal prevalence, mostly a history of trauma or infection	Acute onset, chills, high fever, skin hemorrhagic spots in the trunk and limbs	Increased WBC count, positive urine protein, positive blood culture	Pulmonary consolidation, pleural effusion, pneumatosis of intestinal wall, free gas in the abdominal cavity, encephalitis, brain abscess
Urinary system infection	No certain seasonal prevalence	Fever, abdominal pain, lumbar percussive pain, nausea, vomiting, facial edema, eyelid edema, urinary irritation signs	Unobvious early renal insufficiency, positive urine protein, RBC, WBC, pyocytes, and casts	Enlarged renal volume with coarse margins, abnormal echoes and density of renal parenchyma, pelvicalyceal dilation and effusion

to the patients with EHF. And their prevalence is at almost the same time, during winters and springs. Therefore, their differentiation is necessary. Radiologically, mild cases of influenza, viral upper respiratory tract infection, and common cold are demonstrated with no abnormalities, while severe cases are demonstrated with intrapulmonary infections. X-ray demonstrates most cases with no abnormality, while CT scanning demonstrates patches of consolidation in lungs.

15.9.2 Leptospirosis

Leptospirosis mainly prevails in summers, autumns, and early winters, and the patients all have a history of contact to contaminated water. The disease has an acute onset, with symptoms of chills, high fever, headache, and obvious systemic pain and soreness. The hemorrhagic spots are mainly distributed in the skin of trunk and limbs. Some patients even experience positive urine protein and renal dysfunction. At the early stage of leptospirosis, by dark-field microscopy, the pathogenic leptospiras can be observed in the blood smear. Meanwhile, early medication of penicillin is effective to treat the disease and the conditions rapidly improve after the body temperature returns to normal. The radiological demonstrations of the lesions are in the chest, with pulmonary interstitial changes, intrapulmonary miliary nodules, lobular pneumonia, enlarged heart shadow, dilated superior vena cava, and pleural thickening.

15.9.3 Typhoid Fever

Typhoid fever is an acute intestinal infectious disease caused by typhoid bacillus. Its clinical manifestations include persistent high fever, systemic toxic symptoms, gastrointestinal symptoms, relatively moderate pulse, roseola, hepatosplenomegaly, and leukopenia. By blood and bone marrow cultures, the findings are positive. Radiological examinations demonstrate hepatosplenomegaly, thickened ileocecal wall, enlarged mesenteric lymph nodes, cholecystitis, and swollen appendix.

15.9.4 Acute Gastroenteritis, Food Poisoning, and Acute Bacillary Dysentery

Gastrointestinal EHF tends to be misdiagnosed as acute gastroenteritis, food poisoning, or acute bacillary dysentery. However, acute gastroenteritis, food poisoning, and acute bacillary dysentery commonly occur in summers and autumns and in patients with a history of excessive food intake and drinking or unhygienic food intake. Except for the common symptoms of fever, nausea, vomiting, diarrhea, and abdominal pain, the patients with gastrointestinal EHF show different symptoms, signs, blood and urine routine tests results, and biochemical findings. In addition, the patients with gastrointestinal EHF experience no renal insufficiency and no obvious radiological changes. For some rare cases, gastrointestinal X-ray demonstrates dilated intestinal canal, rapid peristalsis, and intragastric fluid retention.

15.9.5 Acute Abdominal Diseases

Acute abdominal EHF is clinically characterized by acute abdominal pain. The patients experience fever, increased WBC count, obvious abdominal tenderness and rebound pain, and even tense abdominal muscle. Abdominal X-ray demonstrates gastrointestinal distension, and even air-fluid level, which tends to be misdiagnosed as acute abdominal disease. Based on the site and degree of abdominal tenderness and pain, it may be misdiagnosed as acute pancreatitis, gastric perforation, cholelithiasis, cholecystitis, acute peritonitis, and ectopic pregnancy. However, except for the finding of a small quantity of urine protein, these diseases share no commonalities to EHF in aspects of clinical symptoms, physical signs, and changes by blood and urine tests. These diseases are radiologically demonstrated as changes in the gastrointestinal tract and abdominal organs, such as dilation and pneumatosis of intestinal canal, thickened intestinal wall, free gas in abdominal cavity, ascites, acute pancreatitis, and cholecystitis.

15.9.6 Pulmonary Infection

The patients with EHF usually experience obvious pulmonary symptoms and signs. Radiological examinations also demonstrate pulmonary inflammation or infiltrative changes. Thus, in the early stage, EHF can be misdiagnosed as pulmonary infection. For cases with pleural effusion, the disease may even be misdiagnosed as pleuritis. In addition to fever, respiratory symptoms, pulmonary signs, and increased WBC count in peripheral blood, the patients with pulmonary infection experience no skin triple redness sign, no triple pain sign, no renal insufficiency, and no abnormalities in routine blood and urine tests as well as biochemical examinations.

15.9.7 Septicemia

Septicemia usually has an acute onset, with chills, high fever, skin hemorrhagic spots, increased WBC count, and positive urine protein. In cases with hemolytic streptococcus or *Staphylococcus aureus* infections, the patients also experience skin congestion in the face and trunk with flushing appearance, but no skin triple redness sign, no triple pain sign, no bulbar conjunctival edema, and no renal percussive pain. The patients with septicemia commonly experience arthralgia, jaundice and hepatosplenomegaly, and rarely renal dysfunction. Blood culture is positive. Radiological examinations demonstrate lung consolidation, pleural effusion, pneumatosis in the intestinal wall, free gas in abdominal cavity, encephalitis, and brain abscess.

15.9.8 Urinary System Infection

Both acute nephritis and acute pyelonephritis should be differentiated from EHF. Diseases in the acute stage are manifested as fever, abdominal pain, lumbar percussive pain, and positive findings of urine protein, erythrocytes, leukocytes, pyocytes, and casts. Radiological examinations demonstrate enlarged renal volume with coarse margin, abnormal echoes and density of renal parenchyma, as well as pelvicalyceal dilation and effusion.

Further Reading

Chen ZM, Zhang XR, Chen L, et al. Observation of all renal arterial hemodynamics during epidemic hemorrhagic fever by color Doppler ultrasonography. Chin J Med Ultrasound. 2001;17(2):140–3.

Gong Z, Weng J, Zhao Z, et al. The changes in serum antibody level after immunization with HFRS vaccine. Zhonghua Yu Fang Yi Xue Za Zhi. 2000;34(6):351–4.

Guo JY. Prevention and control of newly emerging infectious diseases. Beijing: Peking Union Medical College Press; 2002.

Guo QJ, Zhu XD. Observation of renal lesions during epidemic hemorrhagic fever by color Doppler ultrasonography. Chin J Ultrasound Diagn. 2003;4(7):537–47.

Han D, Liu Z, Han Q, et al. Acute kidney injury in patients with hemorrhagic fever with renal syndrome caused by Hantaan virus: comparative evaluation by RIFLE and AKIN criteria. Vector Borne Zoonotic Dis. 2011;11(6):723–30.

Lin YH. Diagnosis and treatment of epidemic hemorrhagic fever. Beijing: Chinese Medical Science and Technology Press; 2005.

Yang JY, Zong R, Zhang P. Spiral CT diagnosis of multiple organs impairment in the cases with HFRS. Chin J Med Radiol. 2009;17(5):339–42.

Zhang BL, Yang JY. CT and ultrasonographic demonstrations of renal lesions in the cases of hemorrhagic fever with renal syndrome. Chin J Clin Radiol. 2006;17(4):220–2.